Water Resources Research

RESEARCH ARTICLE
10.1029/2018WR022615

Key Points:
- A stream temperature model coupled with a two-layer reservoir module can efficiently simulate temperature for a multireservoir system
- River temperature simulations are generally improved, especially downstream of reservoirs with longer residence times

Supporting Information:
- Supporting Information S1

Correspondence to:
B. Nijssen,
nijssen@uw.edu

Citation:
Niemeyer, R. J., Cheng, Y., Mao, Y., Yearsley, J. R., & Nijssen, B. (2018). A thermally stratified reservoir module for large-scale distributed stream temperature models with application in the Tennessee River Basin. *Water Resources Research*, *54*, 8103–8119. https://doi.org/10.1029/2018WR022615

Received 22 JAN 2018
Accepted 21 SEP 2018
Accepted article online 4 OCT 2018
Published online 19 OCT 2018

A Thermally Stratified Reservoir Module for Large-Scale Distributed Stream Temperature Models With Application in the Tennessee River Basin

Ryan J. Niemeyer[1], Yifan Cheng[1], Yixin Mao[1], John R. Yearsley[1], and Bart Nijssen[1]

[1]Department of Civil and Environmental Engineering, University of Washington, Seattle, WA, USA

Abstract River temperatures affect water quality, power plant cooling, and freshwater ecosystems. Stream temperature models that treat river reaches and reservoirs as well-mixed segments do not capture thermal stratification in reservoirs. To account for the effects of reservoir stratification on downstream water temperatures, we developed a two-layer stratified reservoir module, which was integrated into the River Basin Model (RBM) to simulate river temperature across a river network with multiple large thermally stratified reservoirs. To evaluate the performance of this model configuration compared to RBM without thermally stratified reservoirs, we simulated river temperature in the Tennessee River Basin in the southeastern United States. We simulated land surface hydrologic fluxes using the Variable Infiltration Capacity (VIC) model and routed runoff using the river routing model RVIC. The two-layer model configuration reduced the bias in simulated summer river temperature from 6.7 to −1.2 °C downstream of a reservoir with a residence time of 92 days and from 3.0 to −0.7 °C downstream of a reservoir with a residence time of 8 days. Improvement in fall and winter, when reservoirs tend to be well mixed, is minimal. RBM with the two-layer module also captured the observed longitudinal river temperature variation downstream of a reservoir, with cool temperatures immediately downstream of the reservoir and gradual warming of the river as it flows downstream. Incorporating a simple stratified reservoir module into RBM improves model performance and increases the ability to apply the river temperature model to large basins with multiple large reservoirs.

Plain Language Summary River temperature is important for ecosystem health and water quality. It is affected by natural processes and also by human interventions, such as man-made infrastructure. In particular, the construction of dams has established large and deep reservoirs where the temperature near the surface is warmer during summer than near the bottom. This change of temperature with depth is a natural process, called thermal stratification. Since water is typically released from the deeper reservoir layers, the water temperature downstream of these dams is often cooler during summer than it would have been without dams. This stratification process is well known and has been modeled before, but we are interested in capturing this process in large river systems with many large dams. In this paper, we develop a new component to represent the effects of stratification on reservoir and stream temperature and add it to an existing computer model that simulates stream temperature. We simplify the problem by representing the reservoir as a two-layer system and demonstrate that the model matches the behavior of observed stream temperatures in the Tennessee River Basin. The resulting model is suitable for application over river basins with many reservoirs.

1. Introduction

River temperature influences many aspects of water resources including water quality (Ducharne, 2008; Haag & Westrich, 2002; Ozaki et al., 2003), power plant cooling (Förster & Lilliestam, 2011; Koch & Vögele, 2009), and freshwater ecosystems (Eaton & Scheller, 1996; Ebersole et al., 2001; Lehmkuhl, 1972; Mohseni et al., 2003; Neves & Angermeier, 1990). River temperature in any given reach results from the water and energy balance for that reach and is therefore affected by water resources management. Reservoirs in particular alter river flow by dampening peak and low flows via reservoir storage (McCully, 2001; Rosenberg et al., 2000). Reservoirs are widespread—in the United States reservoir water storage equals 75% of the mean annual runoff of all U.S. rivers (Biemans et al., 2011). Globally, reservoirs increase the time water resides in rivers by approximately 1 month for all rivers on average and 2 months for impounded rivers (Vörösmarty et al., 1997).

Table 1
Examples of Existing Large-Scale Distributed Land Surface and River Temperature Models With Reservoirs

Manuscript	Modeling domain, spatial and temporal resolution	Reservoir simulation scheme	Reservoir stratification?	Stream temperature model evaluation time step and statistics
Li et al. (2015)	Contiguous western United States, 1/8°, daily	In reaches with reservoirs, flow is regulated and cell geometry is enlarged to emulate a reservoir	No	Daily, all NSEs above 0.5 (did not summarize NSEs, only mapped NSE values, therefore includes sites upstream of reservoirs)
van Vliet, Yearsley, Franssen, et al. (2012)	Global, 1/2°, daily	In reaches with reservoirs, cell geometry is enlarged and flow is reduced to emulate a reservoir	No	Daily, average median bias = −0.3 °C; average RMSE = 2.8 °C, average r[a] = 0.88 (across all sites, including upstream of reservoirs)
van Vliet, Yearsley, Ludwig, et al. (2012)	Europe and United States, 1/8°, daily	(Same as above)	No	No model evaluation
Boehlert et al. (2015)	Contiguous United States, sub-8-digit HUC (river segments ~16 km), monthly runoff, hourly river temperature	Two-layer reservoir model with surface energy and diffusion between layers	Yes	No model evaluation
Buccola et al. (2016)	North Santiam River, 559 and 280 km^2 (simulated two basins for inflow), daily	Reservoir energy and flows simulated with CE-QUAL-W2	Yes	Time step not specified, mean absolute error = 0.34 °C, NSE = 0.98 (only compared for 1 year)
This study	Tennessee River basin, 1/8°, daily	Two-layer reservoir model with surface energy and advection and diffusion between layers	Yes	Daily, NSE = 0.84 and 0.95, bias = 0.3 and 0.2 °C, RMSE = 2.5 and 1.7 °C (only for two sites downstream of reservoirs)

Note. NSE = Nash-Sutcliffe efficiencies; RMSE = root-mean-square error.
[a]Pearson correlation coefficient.

Reservoirs modify water temperature in a number of ways and by extension affect downstream river temperature. They increase surface warming by increasing the water surface area as well as the residence time of water in the channel. In spring and summer, surface energy fluxes warm the reservoir surface, resulting in lower-density surface waters and an increase of density with depth that prevents water at different depths from mixing, leading to seasonal thermal stratification (Palmer & O'Keeffe, 1989; Petts, 1986; Poole & Berman, 2001; Prats et al., 2010). In other words, thermal stratification is maintained by a stable thermal structure with high internal stability and low diffusion rates between the top (epilimnion) and bottom (hypolimnion) layers (Bonnet et al., 2000; Fisher et al., 1979; Snodgrass & O'Melia, 1975). Stratification persists until the epilimnion becomes cooler than the hypolimnion, which results in vertical instability and a well-mixed reservoir (Palmer & O'Keeffe, 1989; Petts, 1986; Prats et al., 2010). Thermal stratification is most pronounced in reservoirs with longer residence times, while reservoirs with shorter residence times typically exhibit the well-mixed nature of river water (Prats et al., 2010; Yearsley, 2002). In temperate regions where lower flows often coincide with peak stream temperatures, reservoirs typically release water from the hypolimnion, decreasing downstream peak temperature (Petts, 1986; Ward, 1974; Webb & Walling, 1997). Thermal stratification in reservoirs is an important hydrologic process that needs to be accounted for in river temperature models.

Although a number of distributed river temperature models exist (e.g., Li et al., 2015; Wu, Kimball, Elsner, et al., 2012; Yearsley, 2009, 2012), most large-scale distributed land surface and river temperature models do not include reservoir thermal stratification (Table 1). For example, some large-scale models simulate reservoirs along river networks simply by increasing the size of the discretized river cell and slowing down the flow at the site of the reservoir. This scheme accounts for changes in surface area and travel time but not for vertical thermal stratification (Li et al., 2015; van Vliet, Yearsley, Franssen, et al., 2012; van Vliet, Yearsley, Ludwig, et al., 2012). Studies using such a scheme have successfully simulated river temperature downstream of reservoirs with relatively short residence times without explicit representation of reservoir stratification (Risley et al., 2012; Wu, Kimball, Elsner, et al., 2012; Yearsley, 2002). However, model performance can decline at locations downstream of reservoirs with long residence times. For example, Wu, Kimball, Elsner, et al. (2012) simulated river temperatures over the Pacific Northwestern United States with average Nash-Sutcliffe efficiencies (NSE) of 0.69 across all sites for daily river temperature. However, the Skagit River, in the northwestern part of Washington State, had the lowest NSE of 0.47 due to a relatively large positive model bias. The Skagit River is heavily regulated in its middle reaches with three large reservoirs, the largest of which has an average residence time of 118 days. Downstream of these reservoirs, the river shows a narrow seasonal range in

observed temperature (approximately 4.0 to 10.0 °C), suggesting releases from the cooler hypolimnion of a stratified reservoir. Similarly, Li et al. (2015) simulated distributed river temperatures across the continental United States and had the poorest model performance below Hoover Dam which impounds Lake Mead, a stratified reservoir with a long residence time. As a result, Li et al. (2015) recommended incorporating thermal stratification into distributed river temperature models.

Some distributed models have explicitly simulated thermally stratified reservoirs to improve river temperature simulations. In one example, Buccola et al. (2016) simulated river temperature in a single basin with one reservoir by integrating a spatially coarse land surface model with CE-QUAL-W2 (Cole & Wells, 2015) which reproduced daily river temperature with an NSE of 0.98. CE-QUAL-W2 is one of the existing vertically and horizontally discretized two-dimensional or three-dimensional hydrodynamic reservoir models that can simulate reservoir temperature dynamics in detail (e.g., Bradford & Katopodes, 1999; Chung & Gu, 1998; Cole & Wells, 2015; King, 1993). Other examples include the Water Quality for River-Reservoir Systems (USACE-HEC, 1986; Null et al., 2013) and HEC-5Q (Willey, 1986) models developed by the U.S. Army Corps of Engineers. In these two models, reservoirs are represented by multiple one-dimensional horizontal slices and energy conservation equations are used to calculate vertical temperature profiles. These more complex models can provide insights into the thermal structure of stratified reservoirs. However, practical concerns, including software development, model implementation requirements, and computational cost can make it difficult to integrate complex reservoir models into distributed hydrologic and river temperature modeling systems for large-scale applications. Therefore, large-scale applications will benefit from a simpler reservoir scheme that is able to capture the major thermal characteristics of reservoirs and is at the same time easy to integrate into large-scale hydrologic modeling systems. Some existing studies have attempted such a development. For example, Boehlert et al. (2015) incorporated a simple two-layer reservoir model in their simulations of river water quality across the continental United States. However, their study used a lumped model at coarse spatial and temporal resolution, which prevents detailed evaluation of the performance of their reservoir schemes.

To simulate the impact of thermal stratification on river temperature in large-scale, regional applications more effectively, our objective in this study is to incorporate a two-layer reservoir thermal stratification scheme into an existing distributed land surface and river temperature modeling system and evaluate its ability to reproduce observed reservoir and river temperatures. Our specific objectives are to (a) develop and evaluate a two-layer reservoir temperature model that can capture the effects of seasonal thermal stratification on river temperature downstream of reservoirs; (b) evaluate the performance of this model in simulating river temperature for systems with reservoirs that exhibit thermal stratification; (c) conduct a parameter sensitivity analysis of this reservoir model. The reservoir temperature model was tested using multiyear daily stream and reservoir temperature observations in the Tennessee River Basin in the southeastern United States.

2. Methods

2.1. Model Overview

We developed a stand-alone two-layer stratified reservoir model and then coupled it with an existing river temperature model, the River Basin Model (RBM). RBM simulates the cross-sectionally averaged river temperatures forced by energy fluxes across the air-water interface in advection-dominated river systems (Yearsley, 2009, 2012). For a specific river segment, RBM calculates the river temperature based on surface energy fluxes, tributary mixing, and local source and sink terms such as energy inputs from thermal plants. Energy transfer along the river network is calculated with a semi-Lagrangian numerical method. Yearsley (2012) developed a grid-based version of the RBM model which allows RBM to operate with input from grid-based land surface and hydrologic models. This is the version we used in this study.

2.2. Two-Layer Reservoir Model

Following Chapra (1997), we simplified our model representation of the thermal stratification process by representing the reservoir as two well-mixed horizontal layers. The conceptual model for the reservoir is shown in Figure 1. The two-layer model divides a reservoir into an epilimnion layer and a hypolimnion layer (Figure 1). Each of the two layers is treated as a control volume. The heat balance equations for the epilimnion (equation (1)) and hypolimnion (equation (2)) are the following:

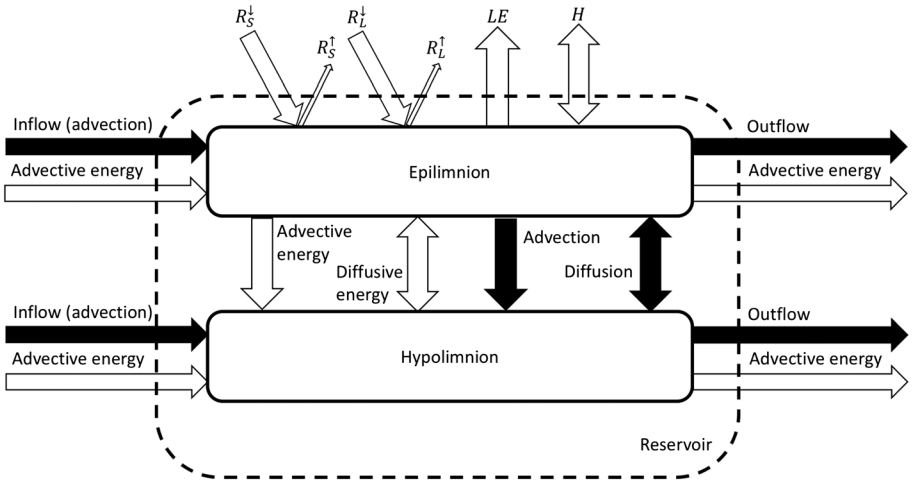

Figure 1. Illustration of the two-layer reservoir module that includes mass and energy fluxes into, out of, and between the two layers. $R_S^{\downarrow}$ is incoming shortwave solar radiation (W/m^2), $R_S^{\uparrow}$ is reflected shortwave solar radiation (W/m^2), $R_L^{\downarrow}$ is incoming longwave radiation (W/m^2), $R_L^{\uparrow}$ is outgoing longwave radiation (W/m^2), *LE* is latent heat flux (W/m^2), and *H* is sensible heat flux (W/m^2).

$$V_e \frac{dT_e}{dt} = Q_{in,e}(T_{in} - T_e) + \upsilon A_S(T_h - T_e) + \frac{A_S J}{\rho_e C_p} \quad (1)$$

$$V_h \frac{dT_h}{dt} = Q_{in,h}(T_{in} - T_h) + Q_{vert}(T_e - T_h) + \upsilon A_S(T_e - T_h) \quad (2)$$

where subscripts *e* and *h* denote variables related to the epilimnion and hypolimnion, respectively, the subscript *in* denotes inflow into the reservoir, and the subscript *vert* denotes the vertical exchange between the epilimnion and hypolimnion. V is the volume of a reservoir layer (m^3), T denotes temperature (°C), Q denotes flow (m^3/s), A_S is the surface area of the reservoir (m^2), J is the net surface energy flux (W/m^2), υ is the rate of heat transfer between the epilimnion and hypolimnion via both eddy and molecular diffusion (m/s), ρ is water density (kg/m^3), and C_p is the specific heat capacity of water (J·kg^{-1}·°C^{-1}). Specifically, $Q_{in,e}$ and $Q_{in,h}$ represent horizontal, upstream flow into the epilimnion or hypolimnion, respectively. Q_{vert} is flow between the epilimnion and hypolimnion. For simplification, we assumed that water flows only from the epilimnion to the hypolimnion and not in the opposite direction. Because we assumed rectangular-shaped reservoirs, the surface area separating the epilimnion and hypolimnion is the same as the reservoir area A_S. The net surface energy flux J (Figure 1) is a function of radiative fluxes (shortwave and longwave radiation) as well as turbulent heat exchange (latent and sensible heat). This surface energy flux was calculated in a manner consistent with that used in RBM for river segments (Yearsley, 2009). Although the epilimnion depth, D_e (m), increases over the summer, D_e is typically smaller than the hypolimnion depth, D_h (m), and summer releases typically occur from the hypolimnion (based on, e.g., Prats et al., 2010, in Europe and data from Tennessee Valley Authority [TVA] in the United States). Here we assumed that the volume of the epilimnion (V_e) remains constant with time and that $Q_{in,e}$ equals Q_{vert}. As a result, the volume of the hypolimnion (V_h) varies with reservoir releases. In the following sections, we describe in detail how the model estimates each of the terms in equations (1) and (2).

Partitioning of total Q_{in} into $Q_{in,e}$ and $Q_{in,h}$ is based on the relative water density of the inflow compared to that of the hypolimnion, where water density is a direct function of water temperature (Weast et al., 1988):

$$\begin{aligned} Q_{in,e} &= (1 - f)Q_{in} \\ Q_{in,h} &= f\, Q_{in} \end{aligned} \quad (3)$$

where

$$f = \begin{cases} 1, & \rho_h < \rho_{in} \\ 0, & \rho_h > \rho_{in} \end{cases}$$

where ρ_h and ρ_{in} are the densities of water of the hypolimnion and inflow (kg/m^3), respectively. Our module allows users to specify f for their particular application. Here we simply set f to 1 or 0, so that Q_{in} either flows into the epilimnion or hypolimnion.

Diffusion is calculated using an empirical equation based on water column stability (Snodgrass & O'Melia, 1975). When a lighter layer overlays a denser layer, the column is very stable. Conversely, when a denser layer overlays a lighter layer, the column is very unstable and turnover will occur. The Brunt-Väisälä frequency N (s^{-1}) is often used to calculate the internal stability of reservoirs (e.g., Alcântara et al., 2010; Casamitjana et al., 2003; Jennings et al., 2012):

$$N = \begin{cases} \sqrt{-1 \times \frac{g}{\rho_e} \times \frac{\rho_e - \rho_h}{\left[\frac{(D_e + D_h)}{2}\right]}}, \rho_e < \rho_h \\ 10^{-6}, \rho_e > \rho_h \end{cases} \quad (4)$$

where g is the gravitational acceleration (m/s^2), and the remaining terms are as defined before. N is set to 10^{-6} s^{-1} when ρ_e is greater than ρ_h because in this situation the two layers will become completely mixed. We calculated υ based on the empirical equation from Quay et al. (1980):

$$\upsilon = \frac{10^{m\ \log(N^2)+b}}{z} \quad (5)$$

where m is -0.65 and b is -3.1 when υ and N are in the units described above, which are both empirical constants taken directly or estimated from Quay et al. (1980). The characteristic depth, z, was assumed to be 1 m. Turnover is the process in lakes and reservoirs in which the water column becomes unstable and mixes vertically due to greater density at the water surface (Bonnet et al., 2000; Snodgrass & O'Melia, 1975). We did not explicitly simulate turnover, but υ is large during unstable conditions, which produces a well-mixed reservoir.

In grid-based RBM, we implemented the two-layer reservoir module for grid cells where reservoirs are located, with each modeled reservoir spanning one or more grid cells along the river network (depending on the length of the reservoir). Reservoir releases were determined by water management operations (see section 2.4 for further description). Based on observed reservoir release information for our study region, we assumed that all releases occur from the hypolimnion as long as there is sufficient water in the hypolimnion. When releases exceed the volume stored in the hypolimnion, releases are from the epilimnion. This situation did not occur during the simulations evaluated in this study.

Following the methods described by Yearsley (2009, 2012), river temperature is calculated with a semi-Lagrangian method. At the beginning of the RBM simulation, water temperatures at each river segment and each reservoir are initialized to a constant temperature (for our study area we used 10 °C). To calculate the water temperatures at a certain time step (t) given the temperatures at the last time step ($t-1$), the water parcel at each segment is tracked to its previous upstream location at time $t-1$ depending on flow velocity. Generally, this location is in between two river segment points, in which case the parcel's temperature at $t-1$ is interpolated based on the adjacent segments (Yearsley, 2009). If a water parcel passes through a headwater or reservoir outlet as it is tracked upstream, its temperature is set to the temperature of the headwater or the reservoir release at time $t-1$. Water parcels are then tracked downstream over the period from $t-1$ to t, and their temperatures at time t are calculated following the energy balance equation described by Yearsley (2009, 2012):

$$\rho C_p \frac{d(T_{nom}\, A_X)}{dt} = S + \frac{\rho C_p Q_{trib} T_{trib}}{D} \quad (6)$$

where T_{nom} is the water temperature for a specific parcel (°C), A_x is the cross-sectional area of the stream (m^2), S is a source term (e.g., thermal plant input; J·s^{-1}·m^{-1}), Q_{trib} is flow from a tributary (m^3/s), T_{trib} is the temperature from the corresponding tributary (°C), and D is the depth of the river channel (m).

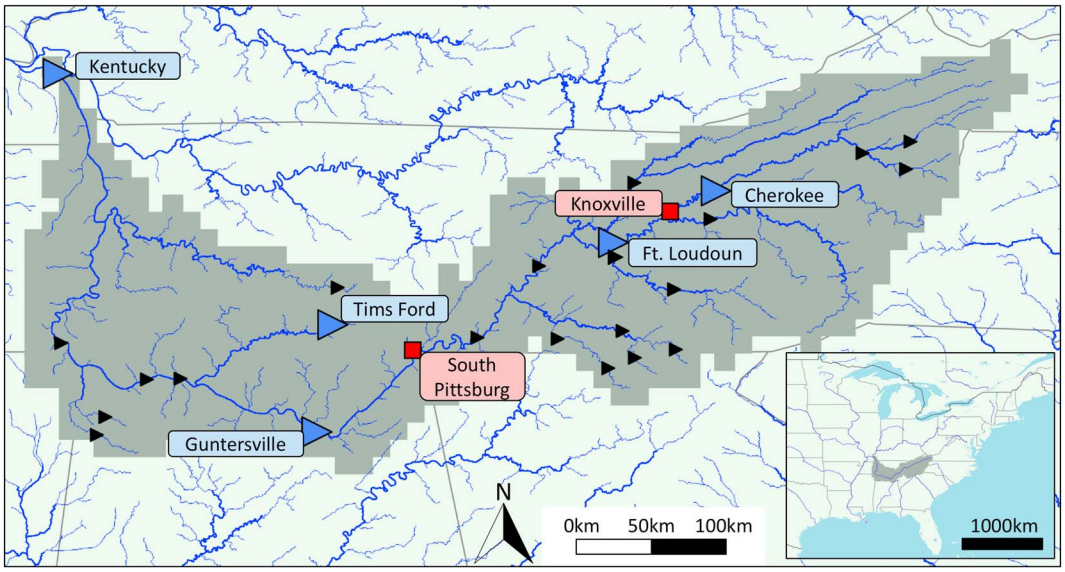

Figure 2. Map of the Tennessee River Basin with the 25 reservoir locations included in the simulations (black and blue triangles show locations of corresponding dams) and downstream U.S. Geological Survey stream temperature measurement sites (red squares). Blue triangles denote dam locations with observed reservoir temperature.

2.3. Study Area and Data Sets

The Tennessee River Basin is located in the southeastern United States with a drainage area of 106,000 km^2 and a mean discharge at the outlet of 2,000 m^3/s (Figure 2). The Tennessee River flows westward into the Ohio River and is its largest tributary. The Tennessee River Basin has 34 major reservoirs, 14 of which have a residence time greater than 50 days (TVA, 2012). The basin has a seasonal climate with warm summer air temperatures and cool winter air temperatures that results in reservoir temperature stratification in the summer for reservoirs with longer residence times.

We compared the simulated river temperatures from RBM with observed river temperature from 20 selected U.S. Geological Survey (USGS) stream sites (USGS, 2018a; Table S1 in the supporting information). These 20 sites were selected because they have both streamflow and stream temperature observations for the simulation time period, and they are located on rivers large enough to be represented at our model resolution. Two sites of particular interest are Knoxville and South Pittsburg (Table 2 and Figure 2), since they are immediately downstream of a reservoir. The other 18 USGS stream sites are located on rivers with drainage areas ranging from 259 to ~59,000 km^2. We also obtained river temperature measurements at five locations downstream of Tims Ford Reservoir along the Elk River. These temperature measurements were collected during the summer from 2005 to 2012 as part of a biological study of dam releases (Potoka et al., 2016).

We also compared simulated and observed temperature in reservoirs. The TVA measured reservoir temperatures at Cherokee Reservoir, Fort Loudon Reservoir, Kentucky Reservoir, and Guntersville Reservoir for a period of 8 to 10 years. These measurements were taken mostly during April to October on a biweekly basis. Reservoir temperatures were measured near the reservoir outlet and were typically measured every 1 to

Table 2
Summary of Selected Sites With Observed River Temperature Data

USGS site city and state	Simulated reservoir immediately upstream of site, river distance downstream (km)	Reservoir volume (m^3)[a]	Mean annual flow (m^3/s)[a]	Drainage area above dam (km^2)	Reservoir residence time (days)[a]	Total days of measurements (days)
Knoxville, TN	Cherokee reservoir, 74	1.9×10^9	127	8.9×10^3	92	2,074
South Pittsburg, TN	Chickamauga reservoir, 85	9.1×10^8	962	5.4×10^4	8	2,587
Multiple sites	Tims Ford reservoir, multiple	6.5×10^8	27	1.4×10^3	240	2,054[b]

Note. USGS = U.S. Geological Survey.
[a]Based on data from Tennessee Valley Authority (2012). [b]Averaged across all five sites and years before end of simulation period at end of 2010.

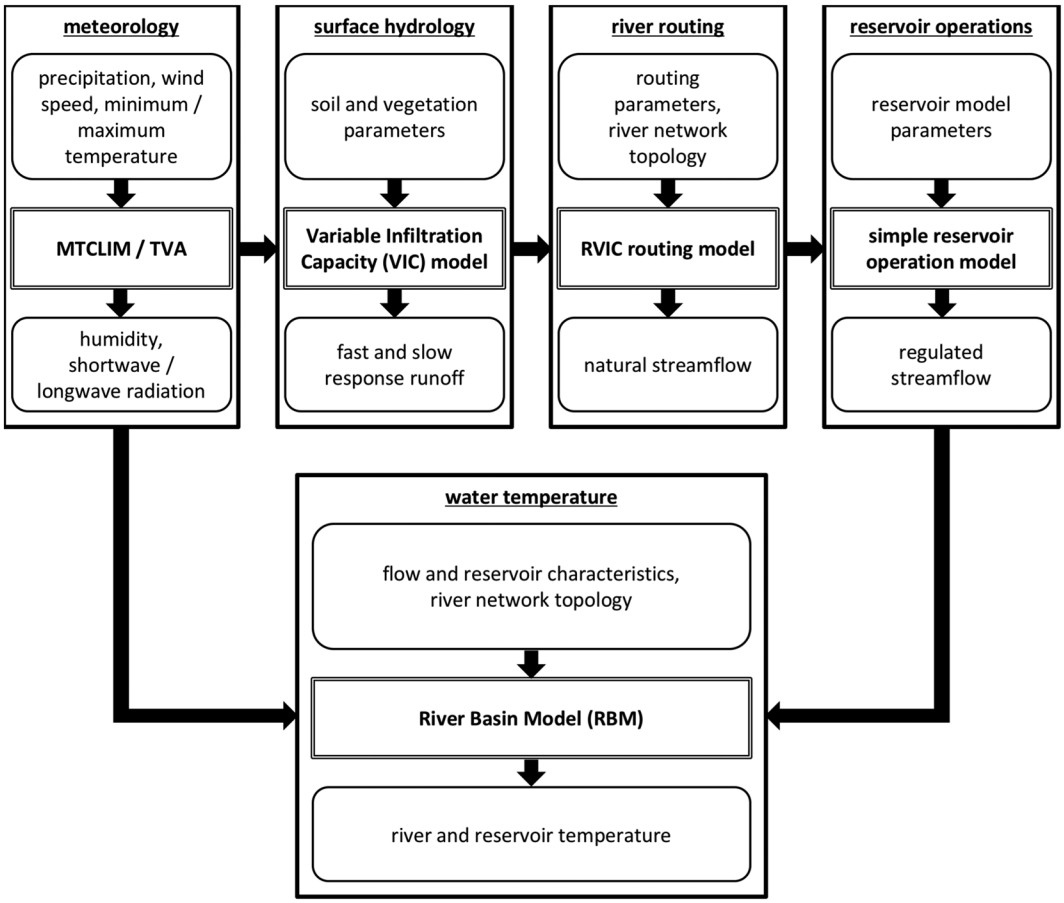

Figure 3. Model framework of the study.

2 m of depth. We determined the typical depth of the thermocline (the separation of the epilimnion and the hypolimnion) in the summer by visually evaluating the measured vertical temperature profiles. For both river and reservoir temperatures, we compared observations with simulated results in terms of the bias and root-mean-square error (RMSE).

We used the gridded daily meteorological data set from Maurer et al. (2002) to provide daily precipitation, minimum and maximum temperatures, and wind speed for the period 1949–2010. Other meteorological forcing variables required by RBM and/or the hydrologic models, including shortwave and longwave radiation, air pressure, and relative humidity, were generated using the MTCLIM algorithms (Bohn et al., 2013; Hungerford et al., 1989; Kimball et al., 1997; Thornton & Running, 1999) and the TVA algorithm (TVA, 1972).

2.4. Modeling Framework

To evaluate the performance of RBM with the two-layer stratified reservoir representation, we conducted two sets of simulations of river and reservoir flow and temperature:

1. RBM with the two-layer reservoir module as described in section 2.2. This simulation is labeled as RBM-2L hereafter;
2. RBM with reservoir representation, but with the two-layer stratification turned off. Instead, we treated each reservoir as a continuously stirred reactor and calculated a single energy balance for the entire reservoir. This simulation is labeled as RBM-NS (denoting no stratification).

Figure 3 shows the modeling framework for our study, which provides flow and energy input variables for both RBM-2L and RBM-NS. This modeling framework is similar to previous Variable Infiltration Capacity (VIC)-RBM studies (van Vliet, Yearsley, Franssen, et al., 2012; Yearsley, 2012).

We simulated surface energy fluxes, hydrology, and river temperature in the Tennessee River Basin at 1/8° spatial resolution from 1949 to 2010. We configured the VIC land surface model (Liang et al., 1994) and linked it with the routing model, RVIC (Hamman et al., 2017), to simulate naturalized streamflow (i.e., flow as if no reservoirs or other human impacts exist), and then simulated the reservoir operation to calculate regulated flow (i.e., flow with reservoir impacts) using a simple reservoir operation model. VIC has been widely used for large-scale hydrological studies in a variety of hydroclimates (e.g., Adam & Lettenmaier, 2008; Clark et al., 2015; Nijssen et al., 2001; Wu et al., 2007). The VIC model was forced with the same meteorological inputs as RBM inputs. Fast and slow response runoff generated by VIC for each grid cell was routed through the river network by the RVIC river routing model, resulting in naturalized streamflow at all flow locations. We then implemented a simple reservoir operation model. At each reservoir, we used historical reservoir storage data from TVA (2012, 2016) to construct a reservoir rule curve to guide releases and imposed maximum and minimum release constraints associated with flood control and environmental flow requirements. Reservoir storage was initialized according to this rule curve, and reservoir releases responded dynamically to inflows and storage levels, subject to the flow constraints. In the simple reservoir operation model, reservoir operation was simulated from upstream reservoirs to downstream ones, so that the impact of upstream reservoir regulation is propagated downstream.

The RBM model (both RBM-2L and RBM-NS) simulated daily river temperatures in the river network discretized to 1/8° model grid cells. The gridded flow direction information was obtained from Wu, Kimball, Li, et al. (2012). In total, 25 major reservoirs were considered in the model. Run-of-river reservoirs were not included in our modeling system since reservoir storage for these reservoirs is relatively small. Reservoir geometries were obtained from the TVA including reservoir location, length, and surface area (TVA, 2012). Mean reservoir width was calculated as reservoir surface area divided by reservoir length. For simplicity, reservoir width and length were kept constant over time. Reservoir depth was calculated from reservoir storage simulated by the simple reservoir operation model. Reservoirs span one or more grid cells depending on the reservoir length obtained from TVA (2012). For RBM-2L, the two-layer module was initialized with an epilimnion depth, D_e, equal to 40% of the total depth and thus an hypolimnion depth equal to 60% of the total depth. The relative epilimnion and hypolimnion depths were estimated based on observed temperature profiles in four stratified TVA reservoirs and the Riba-roja reservoir in the Lower Ebro River in Spain (Prats et al., 2010).

Required inputs into RBM, including stream depth, width, and flow velocity, were estimated from simulated regulated flow based on empirical relationships developed by Leopold and Maddock (1953) and Chapra (1997):

$$D = aQ^b \tag{7}$$

$$w = cQ^d \tag{8}$$

where Q is regulated flow on a given day and grid cell (m^3/s); D is flow depth (m); w is flow width (m); and a, b, c, and d are empirical parameters. Here we assumed constant values for these four parameters over the whole study domain. We fit these constants using historical field measurements of hydraulic cross sections at 3,330 measurement locations throughout the Tennessee River Basin (USGS, 2018b), including discharge, stream channel width, cross-sectional area, and flow velocity. The fitted parameter values are the following: $a = 0.408$, $b = 0.392$, $c = 4.346$, and $d = 0.520$. Once D and w were calculated, flow velocity, v (m/s), was then calculated as

$$v = \frac{Q}{wD} \tag{9}$$

For both RBM-NS and RBM-2L, hydraulic data are not needed at reservoir grid cells since the reservoir module is used for those grid cells instead.

Headwater temperature was estimated with a nonlinear regression model that calculates daily headwater temperature from air temperature (Mohseni et al., 1998):

$$T_{\text{stream}} = \mu + \frac{\alpha - \mu}{1 + e^{\gamma(\beta - T_{\text{air}})}} \tag{10}$$

where μ, α, β, and γ are empirical parameters. We assumed constant values for these parameters throughout the whole river basin and fit the parameters based on stream temperature and daily mean air temperature at

the corresponding grid cell. Stream temperature observations at 18 USGS stream temperature sites in the Tennessee River Basin were used for this purpose. All 18 sites were close to headwater locations and unaffected by reservoir operations. The fitted parameter values are the following: $\alpha = 27.18$, $\beta = 13.39$, $\gamma = 0.18$, and $\mu = 0$. Although thermal effluents from thermoelectric power plants occur in the Tennessee River Basin, we did not account for thermal discharge in this study.

2.5. Two-Layer Model Sensitivity Analysis

We conducted a sensitivity analysis to evaluate the sensitivity of the two-layer reservoir module to its parameters. Initial sensitivity experiments (not shown) showed that the model was particularly sensitive to the relative depths of the epilimnion and hypolimnion. To analyze the impact of this partitioning on reservoir energy dynamics, we conducted a series of sensitivity experiments using the model setup for Cherokee Reservoir. RBM was implemented from 1949 to 2010 for the Holston River Basin with the same modeling framework and meteorological forcings described in section 2.3. Cherokee Reservoir is located on the Holston River upstream of its confluence with the Tennessee River. We conducted seven simulations, in which the initial ratio of the epilimnion depth to the total depth (D_e/D_T) was varied from 0.1 to 0.7 with 0.1 increments. We then investigated the response of the daily change in the epilimnion temperature (ΔT_e), the daily change in the hypolimnion temperature (ΔT_h), and the depth-averaged surface energy input (J).

3. Results

3.1. Discharge

Discharge simulations by VIC, RVIC, and the simple reservoir operation model captured the seasonal peaks and changes in flow with precipitation events and dry periods (time series not shown). The median NSE values at the 20 USGS stream sites are 0.53 and 0.71 for daily and monthly time series, respectively. The median RMSE and median normalized RMSE for mean monthly flows at these 20 sites are 7.28 m^3/s and 0.53, respectively. The median relative bias for streamflow at these 20 sites is 4.6%. For the South Pittsburg gauge, which is located downstream of Cherokee Reservoir, the daily and monthly NSEs are 0.53 and 0.76, respectively. RMSE and normalized RMSE for mean monthly flows at this site are 260 m^3/s and 0.24, respectively. Relative bias for this site is −10.9%.

3.2. Reservoir Temperature

Simulated and observed reservoir temperatures for four TVA reservoirs are shown in Figure 4. The top two rows show the simulated reservoir temperatures at four reservoirs based on RBM-2L and RBM-NS (averaged over all depths), respectively. For both RBM-2L and RBM-NS, a warm bias exists across all reservoirs, but overall reservoir temperatures simulated by RBM-2L outperform those by RBM-NS. Specifically, the bias is greater for RBM-NS, especially at Cherokee Reservoir, which has the longest residence time among the four reservoirs. Daily RMSE values, averaged over all four sites, for RBM-2L and RBM-NS are 1.7 and 4.8 °C, respectively. Comparing all four reservoirs, RBM-NS performs the worst at Cherokee Reservoir, with an RMSE of 7.5 °C and a bias of 6.0 °C. This reservoir also displays the largest relative improvement when thermal stratification is considered with an RMSE of 2.3 °C and a bias of 1.3 °C by RBM-2L.

The bottom two rows in Figure 4 show the simulated reservoir temperatures from RBM-2L averaged over the epilimnion and the hypolimnion, respectively. In general, the simulated values capture the temperature differences between the two layers, but the modeled epilimnion temperatures show a slight warm bias at all reservoirs, while the hypolimnion temperatures show a slight cool bias.

Comparing RBM-2L and RBM-NS across the 25 reservoirs (not shown), RBM-2L consistently produces cooler summer reservoir temperatures than RBM-NS. Average simulated mean August reservoir temperature after 1980, the year the last reservoir we simulated was constructed, is 5.5 °C cooler in RBM-2L than in RBM-NS. For the 12 reservoirs with an average residence time above 50 days, the mean August reservoir temperature is 7.6 °C cooler in RBM-2L than in RBM-NS.

We also compared the turnover dates simulated by RBM-2L with observed turnover dates for each year for the four reservoirs (Figure 5). We assumed that thermal stratification was characterized by a temperature difference of least 0.5 °C between the epilimnion and the hypolimnion. Reservoir temperatures were measured at irregular intervals, and Figure 5 shows the time period during which turnover occurred based on the last

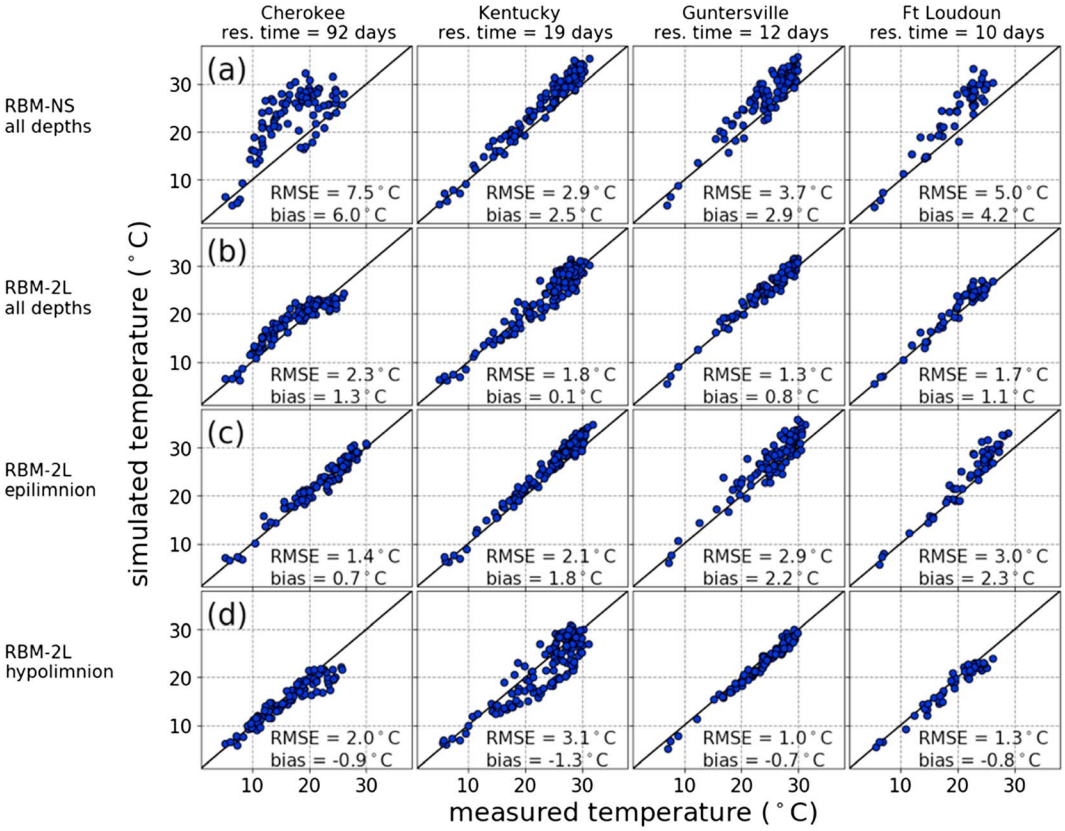

Figure 4. Simulated versus measured reservoir temperature from both RBM-NS (row a) and RBM-2L (row b). Each data point in the figure is one measurement, mostly biweekly during the period April–October. The bottom two rows show the epilimnion (row c) and hypolimnion (row d) temperatures from RBM-2L. Observed epilimnion (hypolimnion) temperatures are calculated by averaging the temperature measurements for the upper 40% (bottom 60%) of the total observed reservoir depth. RBM = River Basin Model; RMSE = root-mean-square error.

measurement before and the first measurement after turnover. To calculate the time lag between the observed and simulated turnover dates, we used the midpoint of the observation interval for comparison with the simulated turnover date. In some years at some reservoirs, observations ended before turnover occurred, in which case we extended the background pattern in Figure 5 from the dates of the last observation to the right side of the figure. Because of the lack of an observed turnover date for these cases, these years were excluded from our lag calculations between observed and simulated turnover dates. Observed turnover occurred between 18 June and 27 October, while simulated turnover dates have a narrower range (between 8 August and 13 October). In general, RBM-2L captures the occurrence of turnover in late summer to midfall. For years for which an observed turnover date is available, RBM-2L predicts turnover 11 days earlier than observed on average, with a mean difference of less than 6 days at Cherokee and Kentucky reservoirs and a mean difference of 23 days at Guntersville. For Fort Loudoun, simulated turnover occurs earlier than observed for most years, with a large outlier of 58 days later in 1990 when observed turnover was uncharacteristically early for this reservoir. Note that the date of the simulated turnover matches the observation better when turnover occurs later in the year, while the match is worse when the turnover happens earlier in the year, perhaps because the simplified two-layer model is not able to represent some complex dynamics of the vertical temperature profile in reservoirs.

3.3. River Temperature

Evaluation statistics of the simulated daily river temperatures are summarized in Table 3. Across all the 20 USGS stream observation sites, the median RMSE is improved from 2.7 °C by RBM-NS to 2.3 °C by RBM-2L (Table 3, first two rows). The annual bias is small for both model versions (Table 3, top two rows).

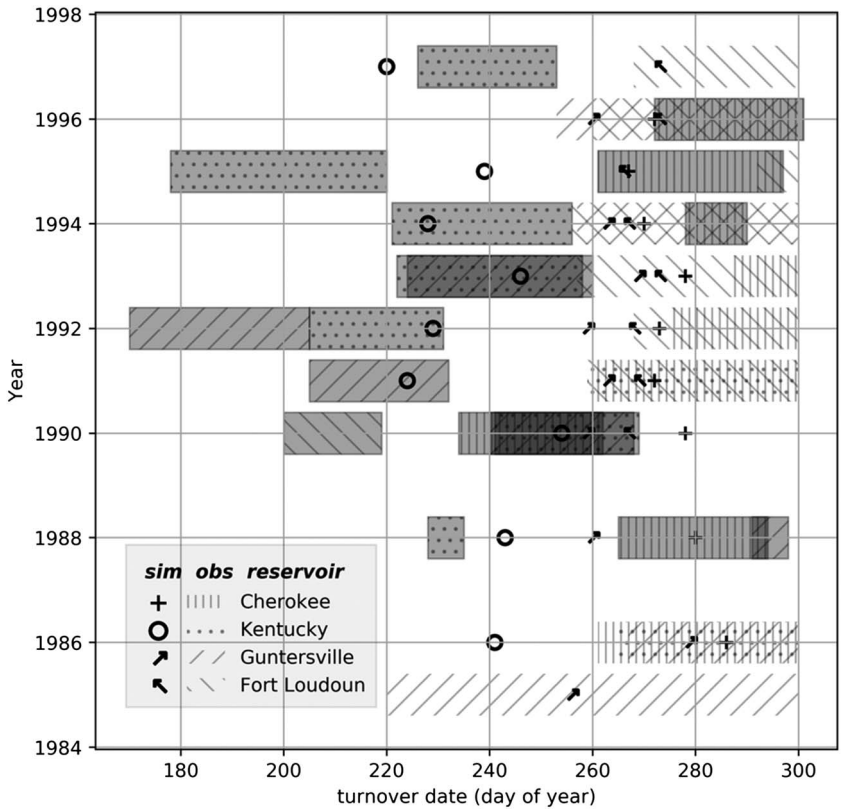

Figure 5. Comparison of simulated versus observed turnover date (i.e., the day of year when turnover occurred) for each year for four reservoirs. Turnover is assumed to occur when the difference between the epilimnion temperature and the hypolimnion temperature is less than 0.5 °C. Markers show the simulated turnover dates. Shaded hatched areas show the time period during which turnover was observed based on the last measurement before and the first measurement after turnover. The unshaded hatched areas represent the situation in which turnover occurred after the last observation. In those cases, the left boundary denotes the day of the last observation and the hatched area is extended to the right boundary at 300 days.

We compared simulated river temperatures of RBM-2L and RBM-NS with observations at Knoxville and South Pittsburg, downstream of Cherokee and Chickamauga reservoirs, respectively (Figure 6). In general, RBM-2L performs better than RBM-NS at both sites, especially during warm seasons. This is consistent with the results shown in Table 3 (last four rows). Overall, RBM-NS overpredicts river temperature, especially in summer, since it is does not account for a cooler hypolimnion in a stratified reservoir. RBM-2L shows a much smaller bias for

Table 3
Statistical Comparison of Daily, Simulated River Temperature Between RBM With Stratification (RBM-2L) and RBM Without Stratification (RBM-NS)

	Annual			Jan–Mar			Apr–Jun			Jul–Sep			Oct–Dec		
Model, USGS Site	Bias (°C)	RMSE (°C)	AMD (°C)	bias (°C)	RMSE (°C)	AMD (°C)	bias (°C)	RMSE (°C)	AMD (°C)	bias (°C)	RMSE (°C)	AMD (°C)	bias (°C)	RMSE (°C)	AMD (°C)
RBM-NS, all selected USGS sites	0.1	2.7	2.2	−1.6	2.3	1.9	1.6	2.7	2.3	1.7	2.5	2.1	−1.2	2.4	2.0
RBM-2L, all selected USGS sites	0.0	2.3	1.9	−1.5	2.2	1.9	0.9	2.4	2.0	1.4	2.1	1.7	−1.2	2.4	1.9
RBM-NS, Knoxville	2.3	5.1	3.8	−1.3	2.2	1.8	3.9	6.0	4.7	6.7	7.4	6.7	−0.9	2.0	1.7
RBM-2L, Knoxville	−1.0	2.5	1.9	−1.1	1.8	1.3	−2.1	3.7	3.0	−1.2	2.3	2.0	0.7	1.3	1.0
RBM-NS, South Pittsburg	1.3	3.3	2.8	−1.0	2.9	2.4	3.5	3.9	3.5	3.0	3.6	3.1	−1.6	2.3	2.0
RBM-2L, South Pittsburg	−0.6	1.6	1.2	−1.5	2.3	1.8	0.2	1.3	0.9	−0.7	1.5	1.1	−0.7	1.6	1.3

Comparisons include bias, RMSE, and AMD. The first two rows of comparison are for locations of all the 20 USGS stream sites (statistics shown are median of all sites). The remaining rows show results at two specific sites, Knoxville and South Pittsburg (Figure 2). RBM = River Basin Model; RMSE = root-mean-square error; AMD = absolute mean difference; USGS = U.S. Geological Survey.

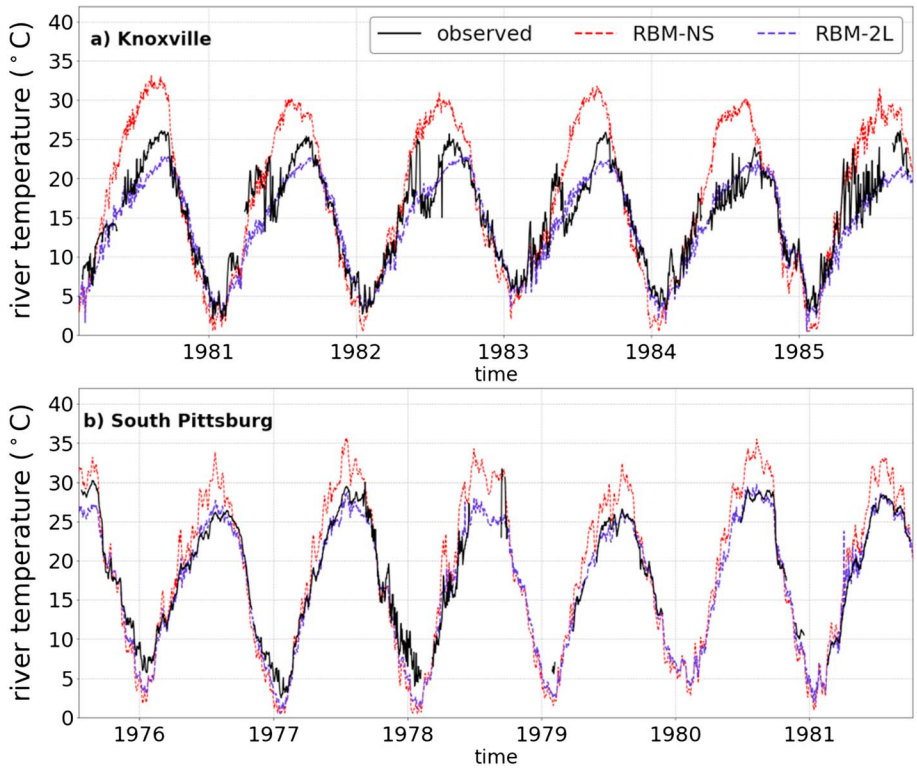

Figure 6. Simulated and observed river temperature at (a) Knoxville gauge downstream of Cherokee Reservoir and (b) at South Pittsburg gauge downstream of Chickamauga Reservoir. RBM = River Basin Model.

the summer river temperature than RBM-NS. The improvement is greater at Knoxville than at South Pittsburg, because their upstream reservoirs have greatly different residence times. Cherokee Reservoir and Chickamauga Reservoir have residence times of 92 and 8 days, respectively, and as a result, there is a greater impact of reservoir stratification on Knoxville river temperature than on the river temperature at South Pittsburg.

Table 3 also shows daily model performance for seasons other than summer at the two stream locations. In general, RBM-2L improves model evaluation statistics for these other seasons as well. Other than summer, spring (April–June) shows the greatest improvement. Fall (October–December) river temperatures are only slightly improved with RBM-2L, since in fall the reservoir is typically well mixed because turnover occurs during this season. Fall is also the season with the best model performance for all model runs and both locations. In winter (January–March), both RBM-2L and RBM-NS show a small low bias for river temperature at both locations.

Comparison between the Elk River temperature observations and simulations downstream of Tims Ford Reservoir reveals that RBM-2L captures the river temperature dynamics as a river parcel moves downstream and the impact of cool reservoir releases diminishes (Figure 7). For example, at a location 22 km downstream of the reservoir, the observed river temperature in the middle of summer typically does not exceed 25 °C (Figure 7e), while the river temperature routinely exceeds this threshold further downstream (e.g., Figure 7a). Peak summer river temperatures increase in the downstream direction. This spatial pattern of observed river temperature is captured well by RBM-2L, while RBM-NS fails to produce this pattern with peak-summer temperature above 30 °C at all locations along the river.

3.4. RBM-2L Sensitivity Analysis

Results of the sensitivity analysis of the initial depth ratio (D_e/D_T) are shown in Figure 8. The three panels show the mean rate of warming or cooling in spring and summer for each depth ratio scenario. The first two panels show the seasonal mean daily warming or cooling (ΔT in °C/day) in the epilimnion (ΔT_e) and the

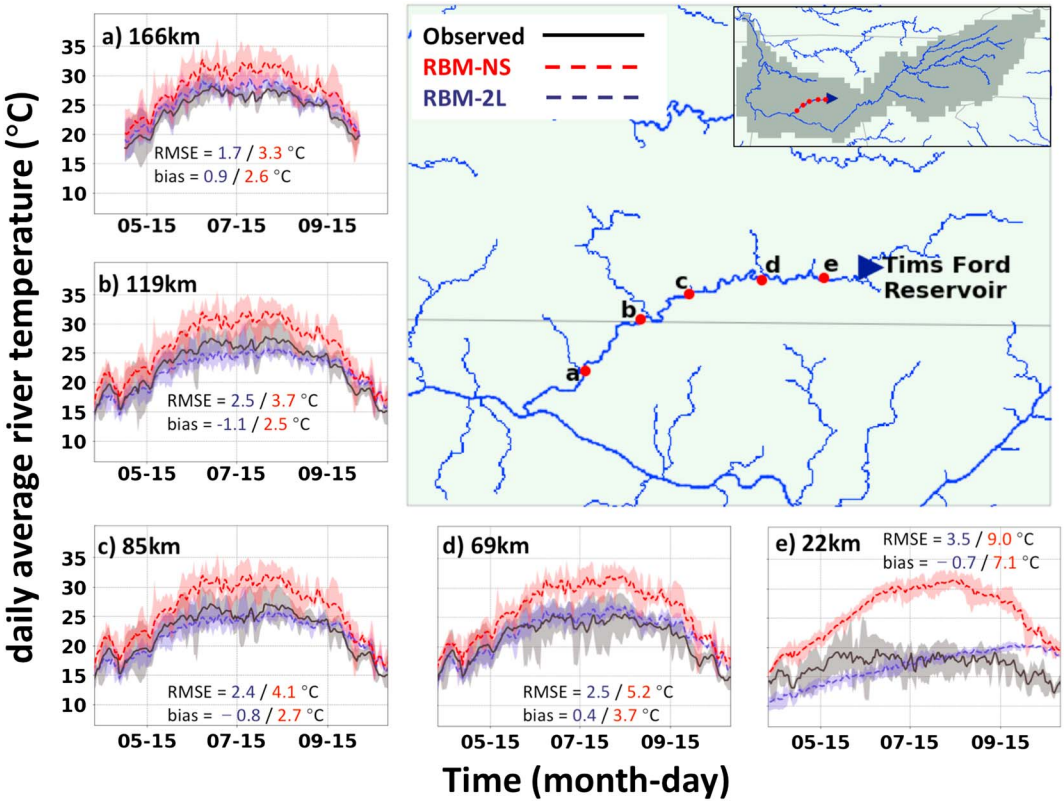

Figure 7. River temperature time series for five sites on the Elk River downstream of Tims Ford Reservoir. Time series show observed and simulated river temperature at each location with shaded area as the maximum and minimum values at each day of year during the period 2005–2010. Only days of year with observations for at least 3 years are shown. The labels in the top left corner of the time series panels show the river distance from the dam location to the observation site. Error metrics (RMSE and bias) are calculated based on daily values. RBM = River Basin Model; RMSE = root-mean-square error.

hypolimnion (ΔT_h), respectively, while the third panel shows the net surface energy input (J) for each depth ratio scenario. We focused on spring and summer because these are the seasons with more significant thermal stratification.

In spring, temperatures in both epilimnion and hypolimnion increase more slowly with a deeper epilimnion (i.e., larger D_e/D_T), as shown by the pink lines in the first two panels of Figure 8. The epilimnion warms more slowly as a result of the greater thermal inertia associated with the larger volume of water. The hypolimnion temperature responds to the temperature increase of epilimnion but is much less sensitive to the depth ratio (D_e/D_T) than the epilimnion temperature.

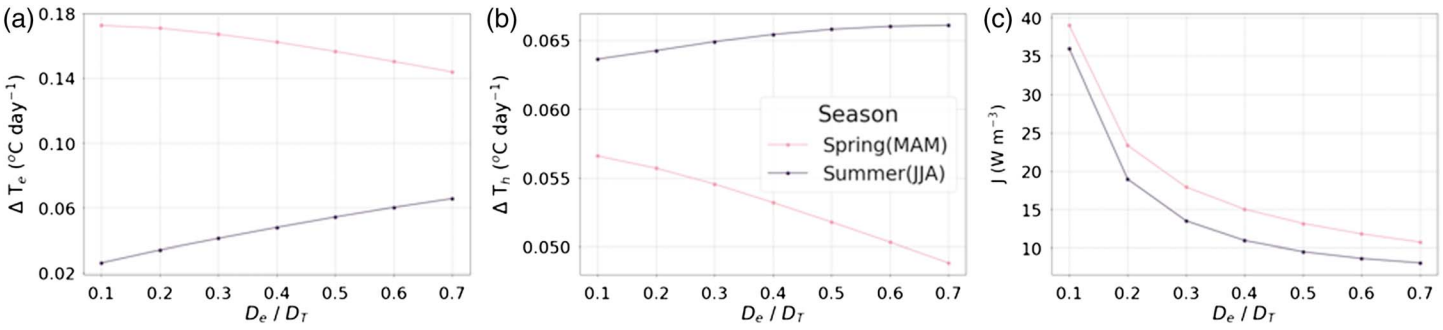

Figure 8. Sensitivity analysis of simulated reservoir temperature at Cherokee Reservoir in response to the ratio of the initial epilimnion depth to the total reservoir depth (D_e/D_T). Sensitivity analyses are for (a) mean seasonal daily change in epilimnion temperature (ΔT_e), (b) mean seasonal daily change in hypolimnion temperature (ΔT_h), and (c) mean seasonal depth-averaged surface energy input (J). Each point indicates the seasonal average value for each variable. MAM = March-April-May; JJA = June-July-August.

In summer, temperatures in both layers show a faster warming rate if the epilimnion is deeper (black lines in the first panels of Figure 8). While a reservoir with a deeper epilimnion warms more slowly, it also cools more slowly at the end of the summer, resulting in a faster overall warming rate during this season. Again, the hypolimnion temperature is less sensitive to the depth ratio (D_e/D_T) than the epilimnion temperature.

The depth-averaged surface energy inputs are greater with a shallower initial epilimnion for both spring and summer (Figure 8c). The total net energy input in summer is smaller than in spring, because increases in downward shortwave and longwave radiation are more than offset by increases in outgoing longwave and increases in turbulent heat fluxes (latent and sensible heat) away from the water surface.

4. Discussion

The two-layer reservoir module incorporated into the RBM model effectively captures seasonal thermal stratification and improves modeled river temperatures in the Tennessee River Basin. RBM-2L captures both the degree and timing of temperature changes in the two layers, as well as that in the entire reservoir on average, which therefore improves simulated river temperatures downstream of reservoirs. The improvement is especially pronounced downstream of reservoirs with longer residence times (e.g., Cherokee Reservoir). Consistent with observations, in RBM-2L released water from the hypolimnion is cooler relative to natural streams during the spring and early summer and warmer during later summer and early fall.

The improvement is moderate at stream locations downstream of reservoirs with relatively short residence times (e.g., South Pittsburg downstream of Chickamauga Reservoir with an 8-day residence time). This finding is consistent with other studies that effectively simulated river temperatures without a stratified reservoir module at stream sites downstream of reservoirs with short residence times (Li et al., 2015; van Vliet, Yearsley, Franssen, et al., 2012; Wu, Kimball, Elsner, et al., 2012; Yearsley, 2002, 2009). At stream locations downstream of reservoirs with longer residence times, past studies have shown worse model performance, as mentioned in section 1. The two-layer stratified reservoir module implemented in this study therefore results in much better simulations of river temperature downstream of reservoirs with longer residence times (e.g., Knoxville downstream of Cherokee Reservoir with 92-day residence time and sites on the Elk River downstream of Tims Ford Reservoir with 240-day residence time). One shortcoming of our model is that it did not capture some of the abrupt increases and decreases in river temperature in spring (Figure 6). By comparing observed releases with these abrupt changes in temperature, it appears that the temperature drops during periods of high releases and increases during periods of low releases. Since our model simulates reservoir releases based on a fixed rule curve estimated from historical median daily releases, it is unable to simulate abrupt temperature changes in response to releases that deviate from the historical median release for that particular day.

In this case study, we assumed that all reservoir releases occurred from the hypolimnion. This assumption may not be valid for reservoirs where active temperature control is possible and water can be extracted from either layer (or a mix). However, the model can be modified easily to accommodate selective withdrawal from either layer (or a mix). Although we applied RBM, as well as the reservoir module, at a daily time scale, in this study, RBM itself has been applied in several studies at a subdaily time step (Sun et al., 2015; Yearsley, 2009).

Errors in simulated river temperature may result from multiple sources. Yearsley (2012) summarized performance metrics in stream temperature simulation studies and reported RMSE values in these studies that ranged from 0.5 to 3.6 °C (RMSE for our study is about 1.7 °C). We performed no exhaustive calibration of model parameters. Our main purpose was to modify an existing stream temperature model (RBM) to account for reservoir effects and to compare the performance of this extended model (RBM-2L) with the original (RBM-NS). Thus, model performance can be improved through further calibration of model parameters. Errors in our simulated stream temperatures do not only result from limitations of RBM-2L and its parameters. We use gridded meteorological forcing data and simulated water fluxes as input to RBM and errors in simulated stream temperature are at least partly inherited from the errors in these inputs. We used simulated rather than observed streamflow as input to RBM, since RBM will typically be used as part of a modeling chain that uses simulated streamflow. Another possible error source is our estimation of headwater temperatures. We used a single set of Mohseni parameters to estimate headwater temperatures for the entire region (Mohseni et al., 1998). This neglect of spatial differences may have led to additional error (Luce et al., 2014; Yearsley, 2009, 2012). However, this error decays as water parcels move downstream and has little impact

on water temperature in large reservoirs. Similarly, our use of simple and generic rules for some of the model component (e.g., we used the same D_e/D_T for every reservoir) ignored much of the detail that makes each reservoir unique. However, qualitatively and quantitatively, RBM-2L outperforms RBM-NS in capturing the effect of reservoirs on downstream stream temperature.

The sensitivity analysis suggests potential ways for parameter calibration and model improvement. For example, in summer, RBM-2L shows a consistent cool bias in simulated river temperature at both Knoxville and South Pittsburg (Figure 6). Calibration of D_e/D_T could potentially improve model performance of both the reservoir temperature and downstream river temperatures. We also conducted a sensitivity analysis to evaluate the impact of reservoir geometry on the simulated epilimnion and hypolimnion temperatures (not shown). We evaluated a series of trapezoidal reservoir cross sections between rectangular and triangular while maintaining the reservoir volume and therefore its thermal mass. Reservoir cross section in RBM-2L had a relatively small effect on the simulated epilimnion and hypolimnion temperatures.

As mentioned in section 1, our finding that a two-layer reservoir module improves the simulation of reservoir and river temperatures is not new. The novelty and contribution of our modeling framework is the integration of a simple stratified two-layer reservoir model into a distributed river flow and temperature modeling system which allows for large-scale, regional simulations with tens or hundreds of individual reservoirs. This type of distributed river temperature model with a sufficiently detailed reservoir representation will especially benefit applications in which a large ensemble of river temperature simulations over a large domain is necessary, such as large-scale modeling studies of future climate impacts on river temperatures.

5. Conclusion

River temperatures impact water resources management and the many benefits that river systems provide. However, human activities such as the construction of dams and the management of reservoir releases in turn affect river temperatures. It is, therefore, essential to account for reservoir operations and reservoir stratification to accurately simulate river temperatures in large river basins that often include many large reservoirs. Multiple highly discretized reservoir temperature models exist that capture the complex temperature dynamics in reservoirs, but these models typically require significant model development, parameter estimation, and computational cost, making application of these models over large-scale domain with numerous reservoirs difficult. A challenge with any large-scale hydrologic modeling effort is to capture all the salient hydrologic processes but retain a model that requires easily obtainable input parameters and reasonable computational cost. Our study accomplishes this by incorporating a simple two-layer reservoir module into an existing hydrologic and river temperature modeling system. By including a two-layer representation of thermal stratification and the dominant energy exchange terms that affect stream temperature, we improve the simulation of both reservoir temperature and downstream river temperature.

The greatest improvement in river temperature simulations occurs at river sites downstream of reservoirs with longer residence times and at sites closer to reservoir outlets. Furthermore, the time of year when river temperature simulation is most improved is in the spring and summer months when reservoir stratification occurs. As a result, the addition of a stratified reservoir will not greatly improve river temperature simulations if the river site of concern is downstream of reservoirs with short residence times, is far downstream of a reservoir, or the period of concern is not principally in the spring or summer. However, many of the world's large rivers include reservoirs with long residence times. Also, peak summer temperatures are often of greatest concern for power plant cooling and aquatic habitats. Therefore, the simplicity of the two-layer reservoir module described here allows for the application of RBM to large regulated river systems to gain scientific insights and improve management of these rivers.

Acknowledgments
This project was funded in part by NOAA grant NA14OAR4310250 and NSF grant EFRI-1440852 to the University of Washington. We also wish to thank the Tennessee Valley Authority for providing data and Tian Zhou (now at Pacific Northwest National Lab) for help with the hydrologic parameter calibration. The code for RBM and the two-layer reservoir module is available at https://github.com/UW-Hydro/RBM/tree/support/10.1029_2018WR022615.

References

Adam, J. C., & Lettenmaier, D. P. (2008). Application of new precipitation and reconstructed streamflow products to streamflow trend attribution in northern Eurasia. *Journal of Climate*, *21*(8), 1807–1828. https://doi.org/10.1175/2007JCLI1535.1

Alcântara, E. H., Bonnet, M. P., Assireu, A. T., Stech, J. L., Novo, E. M. L. M., & Lorenzzetti, J. A. (2010). On the water thermal response to the passage of cold fronts: Initial results for Itumbiara reservoir (Brazil). *Hydrology and Earth System Sciences Discussions*, *7*(6), 9437–9465. https://doi.org/10.5194/hessd-7-9437-2010

Biemans, H., Haddeland, I., Kabat, P., Ludwig, F., Hutjes, R. W. A., Heinke, J., et al. (2011). Impact of reservoirs on river discharge and irrigation water supply during the 20th century. *Water Resources Research*, *47*, W03509. https://doi.org/10.1029/2009WR008929

Boehlert, B., Strzepek, K. M., Chapra, S. C., Fant, C., Gebretsadik, Y., Lickley, M., et al. (2015). Climate change impacts and greenhouse gas mitigation effects on U.S. water quality. *Journal of Advances in Modeling Earth Systems*, *7*, 1326–1338. https://doi.org/10.1002/2014MS000400

Bohn, T. J., Livneh, B., Oyler, J. W., Running, S. W., Nijssen, B., & Lettenmaier, D. P. (2013). Global evaluation of MTCLIM and related algorithms for forcing of ecological and hydrological models. *Agricultural and Forest Meteorology*, *176*, 38–49. https://doi.org/10.1016/j.agrformet.2013.03.003

Bonnet, M. P., Poulin, M., & Devaux, J. (2000). Numerical modeling of thermal stratification in a lake reservoir. Methodology and case study. *Aquatic Sciences*, *62*, 105–124. https://doi.org/10.1007/s000270050001

Bradford, S. F., & Katopodes, N. D. (1999). Hydrodynamics of turbid underflows: I. Formulation and numerical analysis. *Journal of Hydraulic Engineering*, *125*(10), 1006–1015. https://doi.org/10.1061/(ASCE)0733-9429(1999)125:10(1006)

Buccola, N. L., Risley, J. C., & Rounds, S. A. (2016). Simulating future water temperatures in the north Santiam River, Oregon. *Journal of Hydrology*, *535*, 318–330. https://doi.org/10.1016/j.jhydrol.2016.01.062

Casamitjana, X., Serra, T., Colomer, J., Baserba, C., & Pérez-Losada, J. (2003). Effects of the water withdrawal in the stratification patterns of a reservoir. *Hydrobiologia*, *504*(1-3), 21–28. https://doi.org/10.1023/B:HYDR.0000008504.61773.77

Chapra, S. C. (1997). *Surface water-quality modeling*. Long Grove, IL: Waveland Press.

Chung, S.-W., & Gu, R. (1998). Two-dimensional simulations of contaminant currents in stratified reservoir. *Journal of Hydraulic Engineering*, *124*(7), 704–711. https://doi.org/10.1061/(ASCE)0733-9429(1998)124:7(704)

Clark, E. A., Sheffield, J., van Vliet, M. T. H., Nijssen, B., & Lettenmaier, D. P. (2015). Continental runoff into the oceans (1950–2008). *Journal of Hydrometeorology*, *16*(4), 1502–1520. https://doi.org/10.1175/JHM-D-14-0183.1

Cole, T. M., & Wells, S. A. (2015). CE-QUAL-W2: A two-dimensional, laterally averaged, hydrodynamic and water quality model, Version 4.0. Portland State University, Portland, OR, USA.

Ducharne, A. (2008). Importance of stream temperature to climate change impact on water quality. *Hydrology and Earth System Sciences*, *12*(3), 797–810. https://doi.org/10.5194/hess-12-797-2008

Eaton, J. G., & Scheller, R. M. (1996). Effects of climate warming on fish thermal habitat in streams of the United States. *Limnology and Oceanography*, *41*(5), 1109–1115. https://doi.org/10.4319/lo.1996.41.5.1109

Ebersole, J. L., Liss, W. J., & Frissell, C. A. (2001). Relationship between stream temperature, thermal refugia and rainbow trout *Oncorhynchus mykiss* abundance in arid-land streams in the northwestern United States. *Ecology of Freshwater Fish*, *10*(1), 1–10. https://doi.org/10.1034/j.1600-0633.2001.100101.x

Fisher, H. B., List, E. J., Koh, R. C. Y., Imberger, J., & Brooks, N. H. (1979). *Mixing in inland and coastal waters*. New York, NY: Academic Press.

Förster, H., & Lilliestam, J. (2011). Modeling thermoelectric power generation in view of climate change: A reply. *Regional Environmental Change*, *10*(4), 327–338. https://doi.org/10.1007/s10113-009-0104-x

Haag, I., & Westrich, B. (2002). Processes governing river water quality identified by principal component analysis. *Hydrological Processes*, *16*(16), 3113–3130. https://doi.org/10.1002/hyp.1091

Hamman, J., Nijssen, B., Roberts, A., Craig, A., Maslowski, W., & Osinski, R. (2017). The coastal streamflow flux in the Regional Arctic System Model. *Journal of Geophysical Research: Oceans*, *122*, 1683–1701. https://doi.org/10.1002/2016JC012323

Hungerford, R. D., Nemani, R. R., Running, S. W., & Coughlan, J. C. (1989). MTCLIM: A mountain microclimate simulation model; INT-414, Ogden, UT. https://doi.org/10.2737/INT-RP-414

Jennings, E., Jones, S., Arvola, L., Staehr, P. A., Gaiser, E., Jones, I. D., et al. (2012). Effects of weather-related episodic events in lakes: An analysis based on high-frequency data. *Freshwater Biology*, *57*(3), 589–601. https://doi.org/10.1111/j.1365-2427.2011.02729.x

Kimball, J. S., Running, S. W., & Nemani, R. (1997). An improved method for estimating surface humidity from daily minimum temperature. *Agricultural and Forest Meteorology*, *85*(1–2), 87–98. https://doi.org/10.1016/S0168-1923(96)02366-0

King, I. P. (1993). *RMA-10. A finite element model for three-dimensional density stratified flow*. Davis, CA, USA: University of California Davis.

Koch, H., & Vögele, S. (2009). Dynamic modelling of water demand, water availability and adaptation strategies for power plants to global change. *Ecological Economics*, *68*(7), 2031–2039. https://doi.org/10.1016/j.ecolecon.2009.02.015

Lehmkuhl, D. M. (1972). Change in thermal regime as a cause of reduction of benthic fauna downstream of a reservoir. *Journal of the Fisheries Research Board of Canada*, *29*(9), 1329–1332. https://doi.org/10.1139/f72-201

Leopold, L. B., & Maddock, T. Jr. (1953). *The hydraulic geometry of stream channels and some physiographic implications*, (Vol. 252). Washington DC, USA: US Government Printing Office.

Li, H.-Y., Ruby Leung, L., Tesfa, T., Voisin, N., Hejazi, M., Liu, L., et al. (2015). Modeling stream temperature in the Anthropocene: An Earth system modeling approach. *Journal of Advances in Modeling Earth Systems*, *7*, 1661–1679. https://doi.org/10.1002/2015MS000471

Liang, X., Lettenmaier, D. P., Wood, E. F., & Burges, S. J. (1994). A simple hydrologically based model of land surface water and energy fluxes for general circulation models. *Journal of Geophysical Research*, *99*, 14,415–14,428. https://doi.org/10.1029/94JD00483

Luce, C., Staab, B., Kramer, M., Wenger, S., Isaak, D., & McConnell, C. (2014). Sensitivity of summer stream temperatures to climate variability in the Pacific Northwest. *Water Resources Research*, *50*, 3428–3443. https://doi.org/10.1002/2013WR014329

Maurer, E. P., Wood, A. W., Adam, J. C., Lettenmaier, D. P., & Nijssen, B. (2002). A long-term hydrologically-based data set of land surface fluxes and states for the conterminous United States. *Journal of Climate*, *15*(22), 3237–3251. https://doi.org/10.1175/1520-0442(2002)015<3237:ALTHBD>2.0.CO;2

McCully, P. (2001). *Silenced rivers: The ecology and politics of large dams*. London, UK: Zed Books.

Mohseni, O., Stefan, H. G., & Eaton, J. G. (2003). Global warming and potential changes in fish habitat in US streams. *Climatic Change*, *59*(3), 389–409. https://doi.org/10.1023/A:1024847723344

Mohseni, O., Stefan, H. G., & Erickson, T. R. (1998). A nonlinear regression model for weekly stream temperatures. *Water Resources Research*, *34*, 2685–2692. https://doi.org/10.1029/98WR01877

Neves, R. J., & Angermeier, P. L. (1990). Habitat alteration and its effects on native fishes in the upper Tennessee River system, east-central USA. *Journal of Fish Biology*, *37*(sA), 45–52. https://doi.org/10.1111/j.1095-8649.1990.tb05019.x

Nijssen, B., O'Donnell, G. M., Lettenmaier, D. P., Lohmann, D., & Wood, E. F. (2001). Predicting the discharge of global rivers. *Journal of Climate*, *14*(15), 3307–3323. https://doi.org/10.1175/1520-0442(2001)014<3307:PTDOGR>2.0.CO;2

Null, S. E., Ligare, S. T., & Viers, J. H. (2013). A method to consider whether dams mitigate climate change effects on stream temperatures. *Journal of the American Water Resources Association*, *49*(6), 1456–1472. https://doi.org/10.1111/jawr.12102

Ozaki, N., Fukushima, T., Harasawa, H., Kojiri, T., Kawashima, K., & Ono, M. (2003). Statistical analyses on the effects of air temperature fluctuations on river water qualities. *Hydrological Processes*, *17*(14), 2837–2853. https://doi.org/10.1002/hyp.1437

Palmer, R. W., & O'Keeffe, J. H. (1989). Temperature characteristics of an impounded river. *Archiv fuer Hydrobiologie*, *116*, 471–485.

Petts, G. E. (1986). Water quality characteristics of regulated rivers. *Progress in Physical Geography*, *10*(4), 492–516. https://doi.org/10.1177/030913338601000402

Poole, G. C., & Berman, C. H. (2001). An ecological perspective on in-stream temperature: Natural heat dynamics and mechanisms of human-caused thermal degradation. *Environmental Management*, *27*(6), 787–802. https://doi.org/10.1007/s002670010188

Potoka, K. M., Shea, C. P., & Bettoli, P. W. (2016). Multispecies occupancy modeling as a tool for evaluating the status and distribution of darters in the Elk River, Tennessee. *Transactions of the American Fisheries Society*, *145*(5), 1110–1121. https://doi.org/10.1080/00028487.2016.1201002

Prats, J., Armengol, J., Marcé, R., Sánchez-Juny, M., & Dolz, J. (2010). Dams and reservoirs in the lower Ebro River and its effects on the river thermal cycle. In D. Barceló & M. Petrovic (Eds.), *The Ebro River basin* (Vol. 13, pp. 77–95). Berlin Heidelberg: Springer. https://doi.org/10.1007/698_2010_68

Quay, P. D., Broecker, W. S., Hesslein, R. H., & Schindler, D. W. (1980). Vertical diffusion rates determined by tritium tracer experiments in the thermocline and hypolimnion of two lakes. *Limnology and Oceanography*, *25*(2), 201–218. https://doi.org/10.4319/lo.1980.25.2.0201

Risley, J. C., Brewer, S. J., & Perry, R. W. (2012). Simulated effects of dam removal on water temperatures along the Klamath River, Oregon and California, using 2010 biological opinion flow requirements (USGS numbered series no. 2011–1311), Open-File Report. U.S. Geological Survey, Reston, VA.

Rosenberg, D. M., McCully, P., & Pringle, C. M. (2000). Global-scale environmental effects of hydrological alterations: Introduction. *Bioscience*, *50*(9), 746–751. https://doi.org/10.1641/0006-3568(2000)050[0746:GSEEOH]2.0.CO;2

Snodgrass, W. J., & O'Melia, C. R. (1975). Predictive model for phosphorus in lakes. *Environmental Science & Technology*, *9*(10), 937–944. https://doi.org/10.1021/es60108a005

Sun, N., Yearsley, J., Voisin, N., & Lettenmaier, D. P. (2015). A spatially distributed model for the assessment of land use impacts on stream temperature in small urban watersheds. *Hydrological Processes*, *29*(10), 2331–2345. https://doi.org/10.1002/hyp.10363

Tennessee Valley Authority (1972). Heat and mass transfer between a water surface and the atmosphere, *Tennessee Valley Authority*, Norris, TN. Laboratory report no. 14. Water resources research report no. 0–6803.

Tennessee Valley Authority (2012). River operations & renewables data repository, November 2012. Retrieved from TVA internal site, Reservoir Information.pdf.

Tennessee Valley Authority (2016). Tennessee Valley Authority lake levels. https://www.tva.gov/Environment/Lake-Levels. [Accessed 19. December.2016.]

Thornton, P. E., & Running, S. W. (1999). An improved algorithm for estimating incident daily solar radiation from measurements of temperature, humidity, and precipitation. *Agricultural and Forest Meteorology*, *93*(4), 211–228. https://doi.org/10.1016/S0168-1923(98)00126-9

United States Geological Survey (USGS) (2018a). USGS surface-water daily data for the nation. Retrieved from https://waterdata.usgs.gov/nwis/dv/?referred_module=sw

United States Geological Survey (USGS) (2018b). Streamflow measurements for the nation. Retrieved from https://waterdata.usgs.gov/nwis/measurements

USACE-HEC (U. S. Army Corps of Engineers-Hydrologic Engineering Center) (1986). WQRRS Water Quality for River-Reservoir Systems user's manual, Hydrologic Engineering Center, Davis, California.

van Vliet, M. T. H., Yearsley, J. R., Franssen, W. H. P., Ludwig, F., Haddeland, I., Lettenmaier, D. P., & Kabat, P. (2012). Coupled daily streamflow and water temperature modelling in large river basins. *Hydrology and Earth System Sciences*, *16*(11), 4303–4321. https://doi.org/10.5194/hess-16-4303-2012

van Vliet, M. T. H., Yearsley, J. R., Ludwig, F., Vögele, S., Lettenmaier, D. P., & Kabat, P. (2012). Vulnerability of US and European electricity supply to climate change. *Nature Climate Change*, *2*(9), 676–681. https://doi.org/10.1038/nclimate1546

Vörösmarty, C. J., Sharma, K. P., Fekete, B. M., Copeland, A. H., Holden, J., Marble, J., & Lough, J. A. (1997). The storage and aging of continental runoff in large reservoir systems of the world. *Ambio*, *26*, 210–219.

Ward, J. V. (1974). A temperature-stressed stream ecosystem below a hypolimnial release mountain reservoir. *Archiv fuer Hydrobiologie*, *74*, 247–275.

Weast, R. C., Astle, M. J., & Beyer, W. H. (1988). *CRC handbook of chemistry and physics* (Vol. 69). Boca Raton, FL: CRC press.

Webb, B. W., & Walling, D. E. (1997). Complex summer water temperature behaviour below a UK regulating reservoir. *Regulated Rivers: Research and Management*, *13*, 463–477. https://doi.org/10.1002/(SICI)1099-1646(199709/10)13:5<463::AID-RRR470>3.0.CO;2-1

Willey, R. G. (1986). HEC-5Q: System water quality modeling. Davis, Calif.: U.S. Army Corps of Engineers, Hydrologic Engineering Center.

Wu, H., Kimball, J. S., Elsner, M. M., Mantua, N., Adler, R. F., & Stanford, J. (2012). Projected climate change impacts on the hydrology and temperature of Pacific Northwest rivers. *Water Resources Research*, *48*, W11530. https://doi.org/10.1029/2012WR012082

Wu, H., Kimball, J. S., Li, H., Huang, M., Leung, L. R., & Adler, R. F. (2012). A new global river network database for macroscale hydrologic modeling. *Water Resources Research*, *48*, W09701. https://doi.org/10.1029/2012WR012313

Wu, Z., Lu, G., Wen, L., Lin, C. A., Zhang, J., & Yang, Y. (2007). Thirty-five year (1971–2005) simulation of daily soil moisture using the variable infiltration capacity model over China. *Atmosphere-Ocean*, *45*(1), 37–45. https://doi.org/10.3137/ao.v450103

Yearsley, J. R. (2002). Columbia River temperature assessment: Simulation of the thermal regime of Lake Roosevelt. EPA910.

Yearsley, J. R. (2009). A semi-Lagrangian water temperature model for advection-dominated river systems. *Water Resources Research*, *45*, W12405. https://doi.org/10.1029/2008WR007629

Yearsley, J. R. (2012). A grid-based approach for simulating stream temperature. *Water Resources Research*, *48*, W03506. https://doi.org/10.1029/2011WR011515